AIP | Applied Physics Letters

In-situ investigation of spontaneous and plasma-enhanced oxidation of AlN film surfaces

Shigeng Song and Frank Placido

Citation: Applied Physics Letters **99**, 121901 (2011); doi: 10.1063/1.3640219
View online: http://dx.doi.org/10.1063/1.3640219
View Table of Contents: http://scitation.aip.org/content/aip/journal/apl/99/12?ver=pdfcov
Published by the AIP Publishing

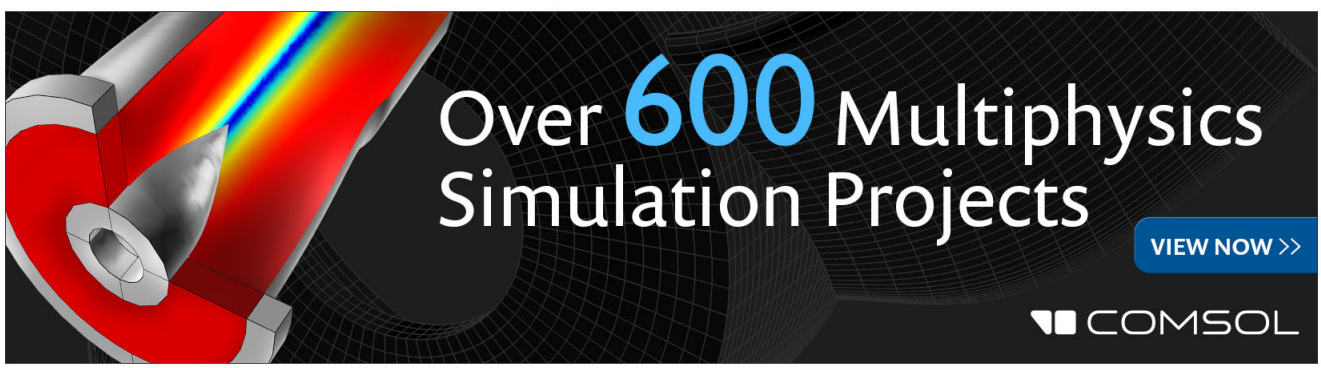

In-situ investigation of spontaneous and plasma-enhanced oxidation of AlN film surfaces

Shigeng Song[a)] and Frank Placido[a)]
Thin Film Centre, SUPA, University of the West of Scotland, Paisley, Scotland PA1 2BE

(Received 10 August 2011; accepted 26 August 2011; published online 19 September 2011)

The oxidation of sputtered AlN thin films on silicon substrates is investigated *in-situ* by high precision, single-wavelength optical monitoring of reflectance for low pressures of oxygen and room temperature conditions. Modelling of spontaneous surface oxidation and plasma enhanced oxidation shows that at the start of oxidation, the amount of available reactants dominates the reaction rate. The Mott potential for plasma enhanced oxidation is found to be much higher than that for spontaneous oxidation, providing explanation of why the oxygen plasma can enhance oxidation of AlN. © *2011 American Institute of Physics*. [doi:10.1063/1.3640219]

AlN is of great interest in many applications. For example, a buffer layer of AlN enhances the structural properties of AlGaN (Ref. 1) improves the strain behaviour of GaN (Refs. 2 and 3) and improves ZnO surface acoustic wave (SAW) devices.[4] AlN films are utilized in SAW devices,[5,6] rugate filters,[7] and has potential for applications in blue-violet emitting diodes, lasers, and ultraviolet light detectors.[8]

Aluminium has a strong affinity for oxygen and there is evidence that this is also true for AlN thin films, with some conversion to Al_2O_3 taking place spontaneously on exposure to oxygen. For example, Mahmood *et al.*[9] showed the spontaneous formation of a thin layer of oxide on exposure to air, using optical fitting of ellipsometric spectra of sputtered AlN films, and confirmed by XPS analysis.[10] In deposition systems where plasma-assisted oxidation takes place, the conversion of nitride to oxide may be even more significant than spontaneous oxidation. In devices based on AlN, the partial conversion to oxide layer has an effect on performance, for example, shifts of luminescence peaks[11] and reduction of the thermal conductivity.[12]

Here, we seek to study the oxidation of AlN thin films in an argon/oxygen atmosphere, with and without microwave-plasma enhancement, using a single-wavelength, reflective monitoring system, and *in-situ* recording of film deposition and subsequent oxidation. Kinetic models of surface oxidation are used to analyse the experimental results.

The *in-situ* investigation of surface oxidation of AlN was carried out in a microwave plasma assisted pulsed-DC sputtering system.[13,14] Appropriate dielectric functions of the AlN and Al_2O_3 films were known from prior experiments. The refractive indices are 1.95 for AlN and 1.65 for Al_2O_3 at 670 nm. This system, is shown in Fig. 1. A temperature-stabilised laser diode system operating at the wavelength of 670 nm provided a very stable, large signal to noise ratio in reflectance mode.[15]

AlN films were deposited using 190 sccm of argon and 30 sccm nitrogen gas. Immediately after deposition of the fresh AlN film, the nitrogen flow was stopped and 30 sccm of oxygen gas (partial pressure of 0.04 Pa) was introduced into the chamber to observe the initial oxidation of the film in argon/oxygen at room temperature. The *in-situ* reflectance was recorded at normal incidence once per second, as the drum and sample (rotating at 60 rpm) pass through the target area, microwave plasma area, and optical monitoring area sequentially.

The measured reflectance during AlN film deposition and oxygen exposure is shown in Fig. 2. The top part of the figure shows the full range of data. The bottom part of the figure shows reflectance at a finer scale for the subsequent steps. The reflectance decreases during AlN deposition. In the region marked stage 1 in Fig. 2, the sputtering process was stopped, the nitrogen was switched off, and oxygen was introduced. A small increase in reflectance was observed, due to initial surface oxidation of the AlN film. This was allowed to reach a stable level before switching on the microwave plasma for stage 2. Early in stage 2, enhanced oxidation of the film causes a further increase in reflectance. This again reaches a stable condition after some time.

Using optical fitting, thicknesses of AlN and Al_2O_3 can be obtained from the measured reflectance, allowing for a 2 nm thick native oxide on the surface of the silicon substrate. The refractive index and extinction coefficient of Si and SiO_2 are well known. Combined with the optical properties of the AlN and Al_2O_3, we have almost all the parameters

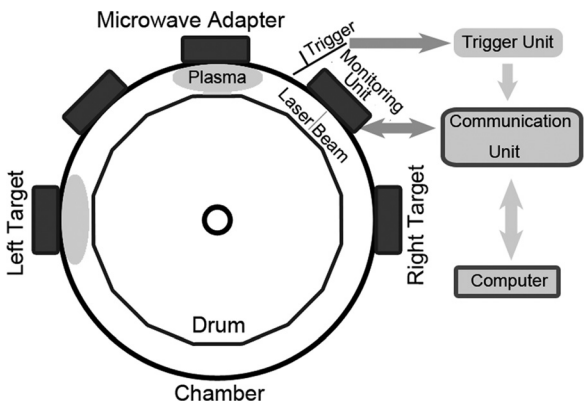

FIG. 1. The arrangement of optical monitoring and deposition system.

[a)]Authors to whom correspondence should be addressed. Electronic addresses: shigeng.song@uws.ac.uk and frank.placido@uws.ac.uk.

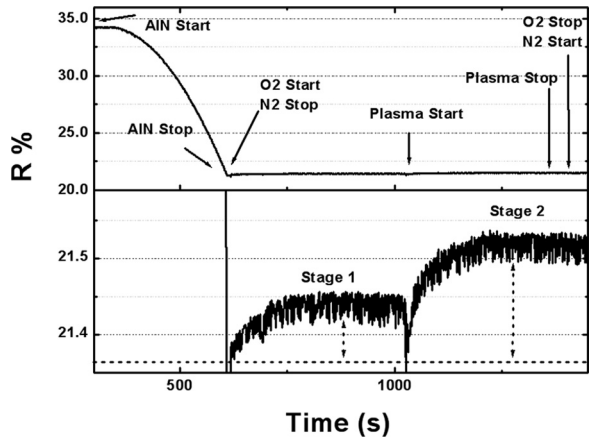

FIG. 2. Reflectance versus time for AlN deposition and surface oxidation.

needed for the simulation and fitting of optical monitor data (assuming refractive index homogeneity in the layers, and Al_2O_3 formed from AlN at surface[9]).

Here, the oxide layer is being formed from the already deposited AlN, therefore, oxide thickness can be determined from the original AlN thickness that is converted into oxide. Thus, an AlN film of thickness d_{AlN} will lead to an oxide layer of thickness d_{Al2O3}, with a thickness correction factor, $f = d_{Al2O3}/d_{AlN}$. As the number of metal atoms per unit area must remain the same before and after oxidation, we have

$$f = \frac{d_{oxide}}{d_{AlN}} = \frac{N_{AlN} \times D_{AlN} \times M_{oxide}}{N_{oxide} \times D_{oxide} \times M_{AlN}}, \quad (1)$$

where D_{AlN} and D_{oxide} are densities, d_{AlN} and d_{oxide} are thicknesses, M_{AlN} and M_{oxide} are molecule weights, and N_{AlN} and N_{oxide} are the number of Al atoms in one molecule of the nitride and oxide layer, respectively. Here, N_{AlN} is 1 and N_{oxide} is 2. Finally, the thickness correction factor is obtained as 0.99.

The typical noise range of unfiltered reflectance measured in this system is 0.044%, as shown in Fig. 2. Calculated reflectance values are 20.972% for 40 nm AlN and 21.199% for 1 nm Al_2O_3 on 39 nm AlN. Thus, the change of reflectance is 0.27% for 1 nm oxide formed from a 40 nm AlN film. Accordingly, the uncertainty in the oxide thickness from our raw data corresponds to ± 0.08 nm ($=0.5 \times 1$ nm $\times 0.044\%/0.27\%$).

Using the information above, we calculate the AlN layer thickness and oxide layer thicknesses as a function of time. The layer stack used for fitting the growing AlN layers was AlN/SiO_2(2 nm)/Si. For the oxidation stage, Al_2O_3/AlN/SiO_2 (2 nm)/Si was used. If the final deposited thickness of the AlN film is d_{final} and the remaining AlN thickness at a given time is d, then the oxide thickness is constrained to be $f(d_{final}\text{-}d)$, where f is the thickness correction factor. A program for fitting the reflectance data was written in MATHCAD. The initial thickness of AlN film deposited was calculated to be 39.32 nm, and we estimate that 0.28 nm of Al oxide was formed by spontaneous oxidation in stage 1, and the thickness grew to 0.63 nm during the plasma-enhanced oxidation in stage 2 (under 4.5 mTorr chamber pressure with Ar gas flow of 190 sccm and O_2 partial pressure of 0.04 Pa, at room temperature).

Spontaneous surface oxidation of AlN (stage 1 in Fig. 2) is a complex process, where oxygen molecules must undergo collision, absorption, diffusion, nucleation, and finally growth to form a complete thin oxide film.[16] The surface oxide layer usually reaches a finite thickness of a few nanometers at room temperature and atmospheric pressure, being limited by the diffusion of oxygen through the new oxide layer to reach unoxidised nitride. In our previous work on kinetic models,[17] equations describing the spontaneous surface oxidation were developed from the following generalized approach of chemical reaction kinetics:

For a first order reaction

$$d(t) = d_1\left[1 - \exp\left(-\frac{t}{\tau}\right)\right] + d_0. \quad (2)$$

For a second order reaction

$$d(t) = d_1\left[1 - \frac{1}{1 + t/\tau}\right] + d_0. \quad (3)$$

The Cabrera-Mott model (CM model)[18] is an important model for surface oxidation that is claimed to be suitable for the growth of native oxides (spontaneous oxidation).[19] The rate of oxide growth is determined by the migration of charged ionic species through the oxide film which is formed in this model by the drive of the so called Mott potential U_M across the oxide film. The oxide growth rate is proportional to the ionic flux. As the oxide layer is very thin in this work, a simplified equation from the CM model is used in this paper

$$\frac{X^2}{A} \cdot \exp\left(-\frac{A}{X}\right) = u \cdot (t + \tau), \quad (4)$$

here τ is an initial time taken to grow the initial oxide thickness, X is the thickness of oxide layer at time, t, and

$$u = V_0 \frac{DC_0}{2a} \quad \text{and} \quad A = \frac{ZeaU_M}{kT}, \quad (5)$$

where V_0 is the oxide volume per migrating ion, D is a diffusion coefficient, 2a is the ion jump distance, Ze is the ion charge, U_M is Mott potential, and C_0 is the concentration of mobile ions.

In this paper, we introduce a combined model of the 2nd order of chemical reaction kinetics and parabolic model, which agrees with the experimental data very well. This is

$$d(t) = d_1\left[1 - \frac{1}{1 + t/\tau}\right] + d_0 + d_2 \cdot t^{1/2}, \quad (6)$$

where d(t) is thickness at time t, τ is time constant, d_1 is the final thickness of initial oxide layer, d_2 is the parabolic growth constant, and d_0 is the initial thickness of the oxide layer. Dimensions for t and τ are s, for d_0, d_1, and d(t) are nm, and for d_2 is $nm/s^{1/2}$.

Equation (2), (3), and (4) are used for the analysis of spontaneous surface oxidation of AlN (stage 1 in Fig. 2).

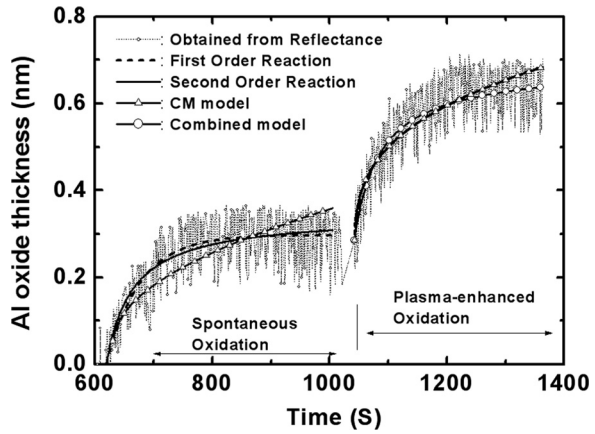

FIG. 3. Al oxide thickness versus time for AlN surface oxidation and fitting results by using various models.

Equations (4) and (6) are used to fit plasma enhanced oxidation of AlN (stage 2 in Fig. 2). All fitting results and experimental data are given in Figure 3. The values of fitting parameters are listed in Table I. The initial thickness can not be zero for Eq. (4) of the CM model, thus, the possible smallest value of thickness from experiment is used as the start thickness for the spontaneous surface oxidation stage.

As shown in Fig. 3, the chemical reaction kinetics models give much better fitting than the CM model for the spontaneous surface oxidation stage. The combined model also fits the plasma enhanced oxidation stage much better than the CM model. The Mott potential across the oxide layer is the main drive of oxide growth in the CM model. If this oxide layer is extremely thin, the field across the oxide layer (provided by Mott potential) will be high and should produce a high oxidation rate. However, the reactants, oxidizing species O_2, O, O^-, or O_2^- etc, cannot support the high reaction rate as the chamber is at low pressure and room temperature in our experiments. This could explain the CM model deviations from the experimental results. However, the CM model still gives some useful information about the oxidation kinetics such as why the plasma enhances oxidation. Plasma enhancement will provide more active reactant species such as O, O^-, and O_2^- but may also induce a higher Mott potential by altering the interface of gases and the oxide layer. The Mott potential can be estimated from the parameter A of Eq. (5), assuming that the ion jump distance is equal to the lattice constant; giving values of 1.57 mV and 36.42 mV at the initial oxidation stage and at the plasma enhanced oxidation stage, respectively. Conclusively, these results show that the Mott potential during plasma enhanced oxidation is much higher than that for spontaneous oxidation, which may be a good explanation for plasma enhancement of AlN oxidation.

TABLE I. The list of fitting parameters.

Spontaneous surface oxidation of AlN (stage 1)	
1st-order	$d_1 = 0.298$, $\tau = 58.177$, $d_0 = 0$
2nd-order	$d_1 = 0.345$, $\tau = 45.776$, $d_0 = 0$
CM model	$A = 0.108$, $u = 2.33 \times 10^{-3}$, $d_0 = 0.053$
Plasma enhanced oxidation of AlN (stage 2)	
Combined model	$d_1 = 0.40$, $\tau = 43.9$, $d_2 = 1.863 \times 10^{-4}$, $d_0 = 0.285$
CM model	$A = 2.000$, $u = 3.87 \times 10^{-5}$, $d_0 = 0.285$

Unit for time is s and for thickness is nm.

[1]X. L. Wang, D. G. Zhao, X. Y. Li, H. M. Gong, H. Yang, and J. W. Liang, Mater. Lett. **60**, 3693 (2006).
[2]C. F. Zhu, J. Q. Xie, W. K. Fong, and C. Surya, Mater. Lett. **57**, 2413 (2003).
[3]A. Ramizy, Z. Hassan, and K. Omar, Mater. Lett. **65**, 61 (2011).
[4]J. Jung, J. Lee, J. Kim, and J. Park, Thin Solid Films **447**, 605 (2004).
[5]M. Clement, L. Vergara, J. Sangrador, E. Iborra, and A. Sanz-Hervás, Ultrasonics **42**, 403 (2004).
[6]L. Brizoual and O. Elmazria, Diamond Relat. Mater. **16**, 987 (2007).
[7]F. Placido, J. Russell, and Z. Gou, SPIE Proc. **2776**, 159 (1996).
[8]G. Iriarte, J. Rodriguez, and F. Calle, Mater. Res. Bull. **45**, 1039 (2010).
[9]A. Mahmood, R. Machorro, S. Muhl, J. Heiras, F. F. Castillón, M. H. Farías, and E. Andrade, Diamond Relat. Mater. **12**, 1315 (2003).
[10]A. Mahmood, N. Rakov, and M. Xiao, Mater. Lett. **57**, 1925 (2003).
[11]G. Slack, L. Schowalter, D. Morelli, and J. Freitas, J. Cryst. Growth **246**, 287 (2002).
[12]G. Slack, R. Tanzilli, R. Pohl, and J. Vandersande, J. Phys. Chem. Solids **48**, 641 (1987).
[13]S. Moh and F. Placido, *Proceedings of the Society of Vacuum Coaters, 47th Annual Technical Conference* (2004), p. 443.
[14]F. Placido and A. Voronov, *Proceedings of the Society of Vacuum Coaters, 45th Annual Technical Conference* (2002), p. 266.
[15]See http://www.ors-ltd.com/pdf/Tech_Noise.pdf, for Low Noise-to-Signal Ratio, Visited on 24th Aug. 2011.
[16]J. R. Davis, *Heat-resistant materials* (ASM International, 1997)
[17]S. Song and F. Placido, Chin. Opt. Lett. **8**, 87 (2010).
[18]N. Cabrera and N. Mott, Rep. Prog. Phys. **12**, 163 (1948).
[19]V. P. Parkhuttik, J. Phys. D: Appl. Phys. **25**, 256 (1992).